From Darkness to Light
ASP Conference Series, Vol. 3×10^8, *2000*
T. Montmerle & Ph. André, eds.

The Orion Star-Forming Region

Lynne A. Hillenbrand & John M. Carpenter

California Institute of Technology; Pasadena CA 91125; USA

Eric D. Feigelson

Pennsylvania State University; University Park, PA, 16802; USA

Abstract. General properties of the Orion star-forming region are discussed, with a focus on the dense Orion Nebula Cluster (ONC). This cluster contains between 2500 and 4500 objects located within a few parsecs of the eponymous Trapezium stars. Its members are aged <1 to a few Myr and encompass the full spectrum of stellar masses <50 $M_\odot$, as well as brown dwarfs detected with masses as low as <0.02 $M_\odot$ (20 $M_{Jupiter}$) thusfar. Recent results from optical, near-infrared, and x-ray studies of the stellar/sub-stellar population associated with this cluster are summarized.

1. Introduction

"Orion" is of course a rather large and daunting topic to which I can not do justice in a single talk. For ample review material I direct your attention to the recent volume on "The Orion Complex, Revisted" edited by McCaughrean, Burkert, & O'Dell (2001, based on a conference held in the summer of 1997).

By way of introduction, let me remind folks that the constellation of Orion is unique in that all of its constituent stars are located at approximately the same distance from the Sun (350-500 pc). This region of the sky is pervaded by a Giant Molecular Cloud usually thought of as two entities, Orion A and Orion B, which together contain 1-3$\times 10^4$ stars aged <1-3 Myr as well as various off-cloud populations aged 3-30 Myr old, including an OB association just to the west which is part of the Gould's Belt system. The spatial extent of current and recent star formation activity is more than 60 degree^2 on the sky. However, the stellar population over this area is still largely uncatalogued. Relative proximity combined with projection ~15-25 degrees out of the plane of the Galaxy means that full census information can be obtained without much of the ambiguity that plagues other similarly interesting star-forming regions located further away and closer to the Galactic plane. The Orion complex contains the nearest Giant Molecular Cloud and also the nearest example of recent massive star formation; as such, it has been the subject of intense study over the past several decades. It continues to be a target of almost every new instrument or technology.

I will spend the majority of my time here discussing results obtained over the past several years on the stellar population of the Orion Nebula Cluster

Region. Older results include those on the Hertzsprung-Russell Diagram for an unbiased sample of ∼1000 stars, the initial mass function, mass segregation, the mean age and age spread, the rate of star formation, and circumstellar disks. Newer results include those on the stellar/sub-stellar mass function as derived from deep near-infrared imaging (in collaboration with John Carpenter) and on the x-rays seen by the Chandra/ACIS instrument (in collaboration with Gordon Garmire, Eric Feigelson, and the rest of the Penn State Chandra/ACIS team). I begin, however, with a summary of what is known globally about the clustering of star formation in the Orion clouds.

2. Clusters in the Orion Star-Forming Region

It is not news that stars form in clusters, perhaps more frequently than not. In fact, two of the more well-studied dense young clusters are located in Orion – the inner ONC (or Trapezium region) with a stellar density of 1-2$\times 10^4$ stars/pc^3, in Orion A, and NGC 2024 with a stellar density of 1-2$\times 10^3$ stars/pc^3, in Orion B. These clusters, and others like them outside of Orion, contain a mix of low- and high-mass stars. They are the proof that stars of all masses (and brown dwarfs too) can and do form in the same place, within <0.05 pc, and at the same time, within <0.5 Myr. That star formation occurs commonly in dense clusters means we ought to consider the potential for mutual influence of cluster stars on each other and on their environments. The relevant physical processes include:

- mergers/coagulation in the post-fragmention, proto-stellar stage;
- enhanced accretion in disks and/or scattering of planetessimals in post-accretion planet-building disks caused by gravitational interactions;
- injection of mechanical energy into the ambient cloud by multiple mis-aligned outflows;
- ionization of the cloud due to high levels of x-ray flux from protostars and young pre-main sequence stars;
- massive star winds and ultraviolet radiation.

Most nearby molecular clouds are in the process of forming stars – at least in a global sense. However, star formation is not happening at all places within these clouds at all times. Rather, it appears to occur in discrete places and at discrete times. This is nicely illustrated in Orion A by the chains of (presumably) protostellar/protocluster cloud cores in the northernmost part of the cloud (Chini et al., 1997; Johnstone & Bally, 1999) which are spatially distinct from the optically revealed ONC, which is in turn spatially distinct from the pockets of clustered optical and still-embedded young stars located further south (Carpenter, 2000; Strom, Strom, & Merrill, 1993). Orion B displays similarly segregated behavior (Carpenter, 2000; Lada et al., 1991). Typical cluster sizes are 0.2-0.5 pc while typical cluster densities are 100-200 stars/pc^3. The full spectrum of cluster parameters remains unquantified: in these same clouds exist the rich ONC and NGC 2024 clusters as mentioned above, but also potentially hundreds of relatively poor, small aggregates which may have dispersed before we

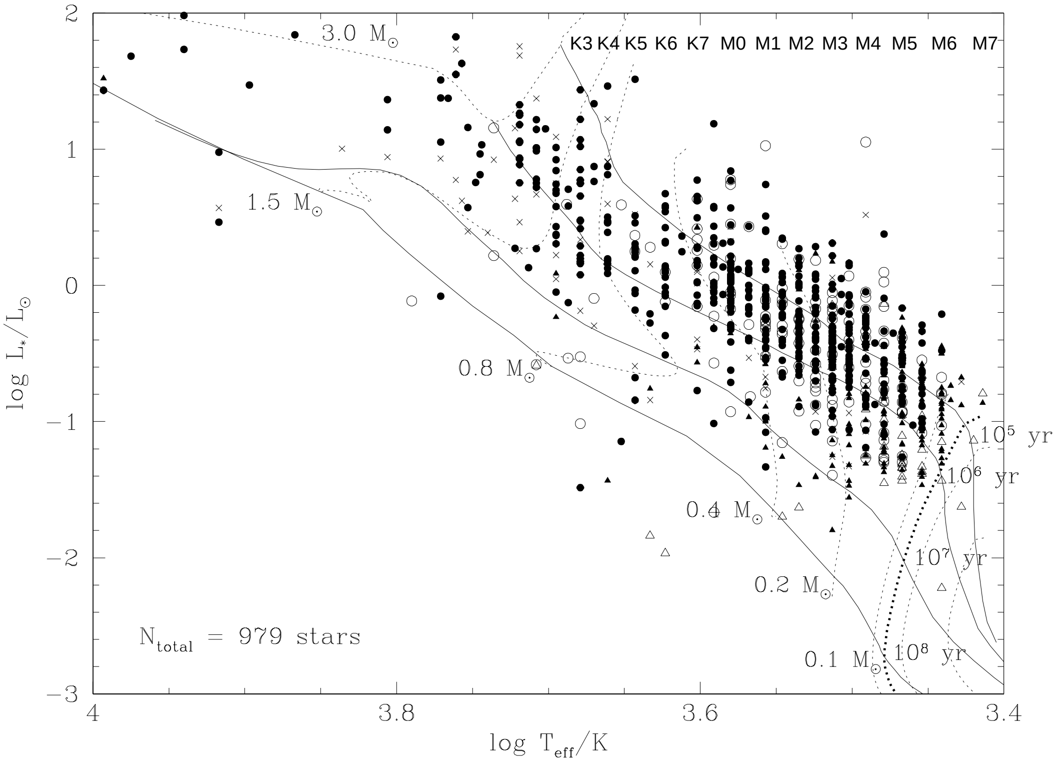

Figure 1. HR diagram for the Orion Nebula Cluster. Triangles indicate lower limits in luminosity. Filled circles/triangles indicate proper motion cluster members plus sources identified as externally ionized; open circles/triangles indicate that no proper motion information is available; crosses indicate proper motion nonmembers. Typical errors are < 0.02 in log T_{eff} and < 0.2 in log L. Superposed are the pre-main sequence evolutionary tracks of D'Antona & Mazzitelli (1997, 1998).

can detect them. Only when it is possible to integrate under a well-established distribution of cluster parameters can we begin to ask questions such as "what is the probability that a star of given mass is born in a cluster of given density."

Studies of both the properties of the clusters and the properties of the stars which constitute them are necessary in order to make progress in this area. I turn now to discussion of some of these details in the ONC itself.

3. Old Results on the Orion Nebula Cluster

Hillenbrand (1997) published a synthesis of census information combined with new optical photometry and spectroscopy for stars within 2-3 pc of the center of the ONC's Trapezium stars. The HR diagram to a completeness limit of I_C=17.5 for this sample is shown in Fig. 1, updated to reflect current transformations from the observations to the HR diagram and also more current theoretical tracks. There remain serious discrepancies at present between different sets of pre-main sequence evolutionary tracks. I have shown the D'Antona & Mazzitelli (1997, 1998) calculations largely because they cover the wide range of effective temperatures and luminosities displayed by the data. Other sets of tracks, e.g.

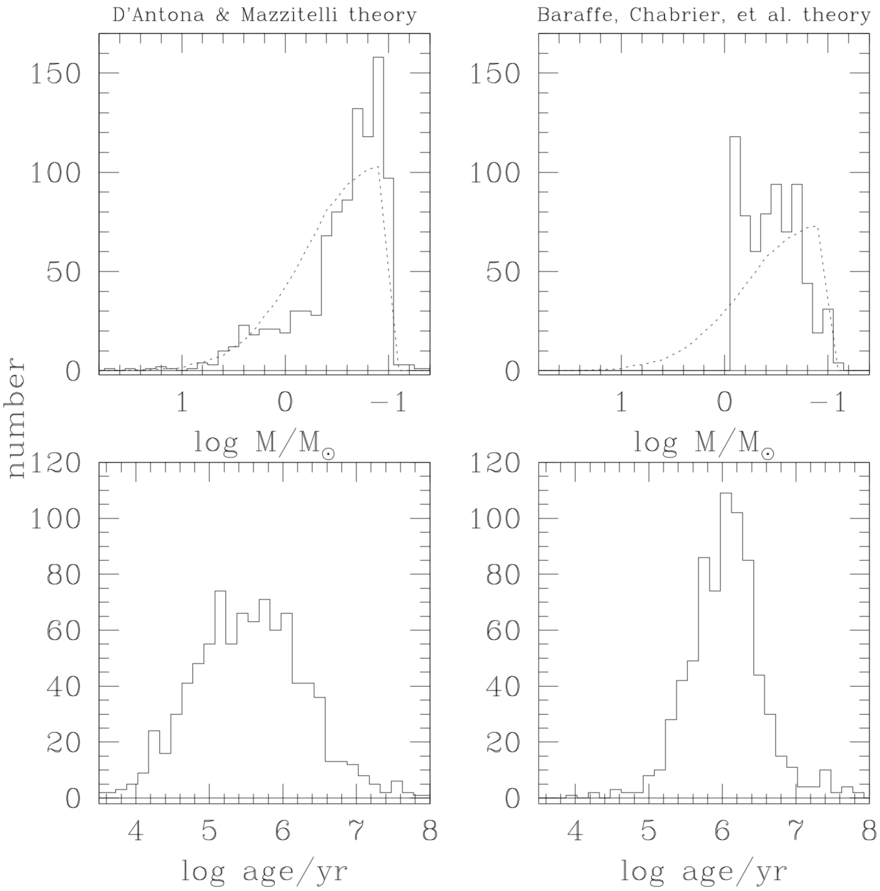

Figure 2. Mass and age distributions for the Orion Nebula Cluster. Left panels show the results from D'Antona & Mazzitelli (1997, 1998) while right panels show the results from Baraffe et al. (1998). Interpolations in mass were restricted to those masses within the boundaries of the tracks while interpolations in age were allowed to exceed the boundaries of the tracks. A Miller-Scalo function truncated at 0.08 $M_\odot$ is shown for reference in the top panels.

those by Siess et al. (2000), Palla & Stahler (1999), and Baraffe et al. (1998), do not cover the full range of the ONC observations (see contributions to these proceedings by these authors for discussion of detailed differences between tracks and the causal physics).

From the ONC data and the theory, one is able to derive quantities such as the stellar mass spectrum and the star formation history. We show in Fig. 2 the mass and age distributions produced by two different sets of theory in order to illustrate their discrepancies. In each of the age panels, the distribution is gaussian in nature, a feature which suggests an increase in the rate of star formation from past to present. In each of the mass panels, the distribution appears as falling towards the hydrogen burning limit, although this turnover nearly coincides with the completeness limit of the data. We pursue the shape of the initial mass function across the hydrogen-burning limit in the next section. From the combined age and mass information, a recent star formation rate in excess of 10^{-3} $M_\odot$/yr is implied.

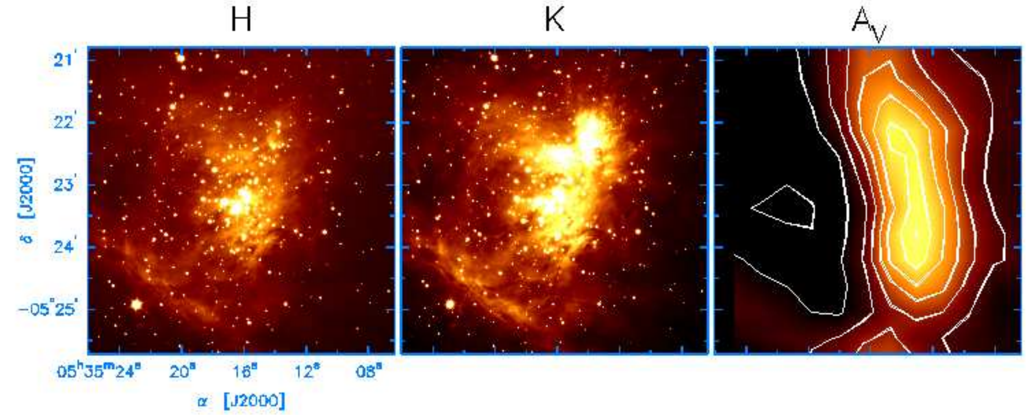

Figure 3. Images of our H and K-band mosaics from Keck/NIRC along with an extinction map derived from the molecular column density data of Goldsmith, Bergin, & Lis (1997). The pixel size of the infrared mosaics is 0.15" and the angular resolution of the extinction map is 50". Contours in the extinction map begin at $A_V = 5$ mag and are spaced at $\Delta A_V = 10$ mag intervals.

4. New Results on the Orion Nebula Cluster

In this section I present more recently obtained results on the stellar/sub-stellar mass function in the inner ONC and regarding the frequency with which x-ray emission is associated with known optical/infrared sources.

4.1. Extension of the Mass Spectrum into the Sub-Stellar Regime

Several groups have attempted recently to quantify the substellar mass function in the inner ONC based exclusively on near-infrared data (Hillenbrand & Carpenter, 2000; Luhman et al., 2000; Lucas & Roche, 2000; see also, Simon, Close, & Beck, 1999). The results of these studies appear quite similar in general terms, which is especially encouraging given the gross differences in technique.

Our study was an imaging survey (see Fig. 3) at K (2.20μm), H (1.65μm), and Z (1.05μm) covering ∼5.1'×5.1' centered on $\theta^1 C$ Ori, the most massive star in the ONC. For the age and distance of the cluster, and in the absence of extinction, the hydrogen burning limit (0.08 $M_\odot$) occurs at K≈ 13.5 mag while an object of mass 0.02 $M_\odot$ has K≈ 16.2 mag. Our photometry is complete for source detection at the 7σ level to K≈17.5 mag and thus is sensitive to objects as low-mass as $0.02 M_\odot$ seen through visual extinction values as high as 10 magnitudes. We used the observed magnitudes, colors, and star counts to constrain the shape of the inner ONC stellar/substellar mass function. To do so, we developed a new technique which assumes the same stellar age and near-infrared excess properties which characterize optically visible stars in this same inner ONC region, and extract a mass function based on probability analysis of the surface density of photometry in the K–(H-K) diagram.

We find that our data are inconsistent with a mass function that rises across the stellar/sub-stellar boundary, as shown in Fig. 4. Instead, we find that the most likely form of the inner ONC mass function is one that rises to a peak

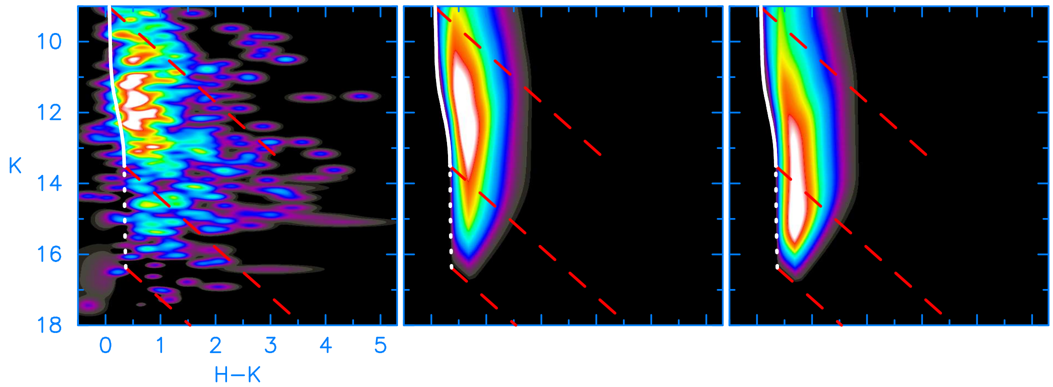

Figure 4. Simulations in Hess diagram format compared with our near-infrared K vs H-K data. The models assume 1) an age distribution which is log-uniform between 0.1 and 1.0 Myr, 2) a near-infrared excess distribution which is a half-gaussian in H-K and related linearly to the monchromatic K excess, and 3) an extinction distribution which is uniform in the interval A_V=0-5 mag. The middle panel shows the log-normal form of the Miller-Scalo mass function while the right panel shows a shallow power law mass function (N(log M) $\propto$ $M^{-0.35}$). Our field-star-subtracted data appear in the left panel. A falling mass function like that of Miller-Scalo better represents the peak in the observed ONC star counts than does an increasing mass function such as the shallow power-law.

around 0.15 $M_\odot$, and then declines across the hydrogen-burning limit with slope N(log M) $\propto$ $M^{0.57\pm0.05}$, as shown in Fig. 5. Our conclusions for the substellar mass function apply to the inner 0.71 pc x 0.71 pc of the ONC only; they may not apply to the ONC as a whole where some evidence for general mass segregation has been found (Hillenbrand & Hartmann, 1998).

4.2. X-rays from Chandra

Pre-main sequence stars are known to display levels of x-ray emission which are 1 to >4 orders of magnitude higher than their counterparts on the main sequence. The x-rays are variable, exhibiting flaring characteristics similar to those of the active sun, and are attributed to $\sim 10^6$ K plasma heated by magnetic reconnection events (see review by Feigelson & Montmerle, 1999).

The Orion region is an old and familiar target of x-ray satellites. The inner ONC region was recently observed during GTO programs with several of the instruments on Chandra. I will describe preliminary results from the Chandra/ACIS (Advanced CCD Imaging Spectrometer) instrument team; see the contribution of Harnden for preliminary results from the Chandra/HRC instrument team. The exquisite spatial resolution (~0.5") and wide field of view of ACIS combined with its low background make it unprecedented for x-ray studies of crowded regions such as the ONC. In Fig. 6 we show the 17 x 17 arcmin^2 ACIS GTO image (48 ksec exposure) of Garmire et al. (2000), claimed to be the richest astronomical x-ray image yet obtained with close to 1000 point sources.

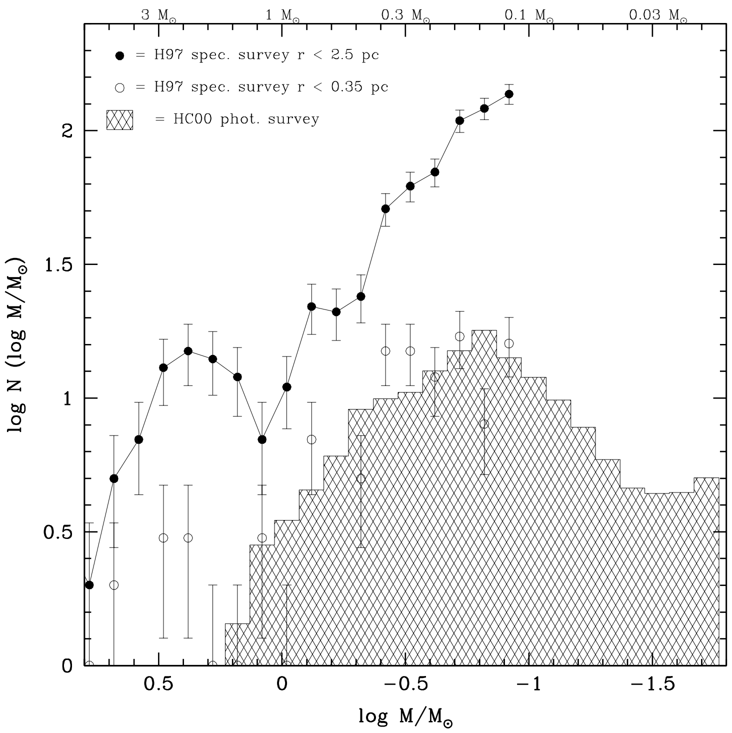

Figure 5. Comparison of the ONC mass spectrum derived from optical spectroscopic techniques (filled and open circles – from data in Hillenbrand, 1997) with that derived using infrared photometric techniques (histogram – from data and analyis of Hillenbrand & Carpenter, 2000). No normalization has been applied to these curves. Note the general agreement between the optical spectroscopic results and the near-infrared photometric results in the mass completeness and the spatial area regimes where they overlap (open circles vs hatched histogram). Note also the disagreement between the shape of the mass spectrum derived for the inner ONC (r<0.35 pc; open circles) vs the greater ONC (r<2.5 pc; filled circles).

Preliminary results based on these data are described in Garmire et al. (2000) with a more detailed paper in preparation (Feigelson et al., 2000). The sensitivity at a limit of 7 photons in the 0.2-8 keV band is to luminosity $\sim 2\times10^{28}$ erg/s assuming kT = 1 keV and little obscuration. A total of 831 sources above this completeness limit and 142 below it have been identified. Thusfar we have cross-correlated the list of ACIS detections with optical and near-infrared sources in the lists of Hillenbrand (1997), Hillenbrand et al. (1998), and Hillenbrand & Carpenter (2000). The optical surveys are complete over the full area of the ACIS image to V$\approx$ 20 mag and several magnitudes deeper in the inner 3 x 3 arcmin^2 based on the work of Prosser et al. (1994). The near-infrared surveys are complete over the full area of the ACIS image to K$\approx$ 13.5 mag and several magnitudes deeper in the inner 5 x 5 arcmin^2. Of the 973 x-ray sources, 860 coincide within <1 arcsec (<2 arcsec in the outermost portions of the x-ray image) with an optical/infrared star. Others are associated with compact radio sources (Menten et al., private communication; Felli et al, 1993; Churchwell et

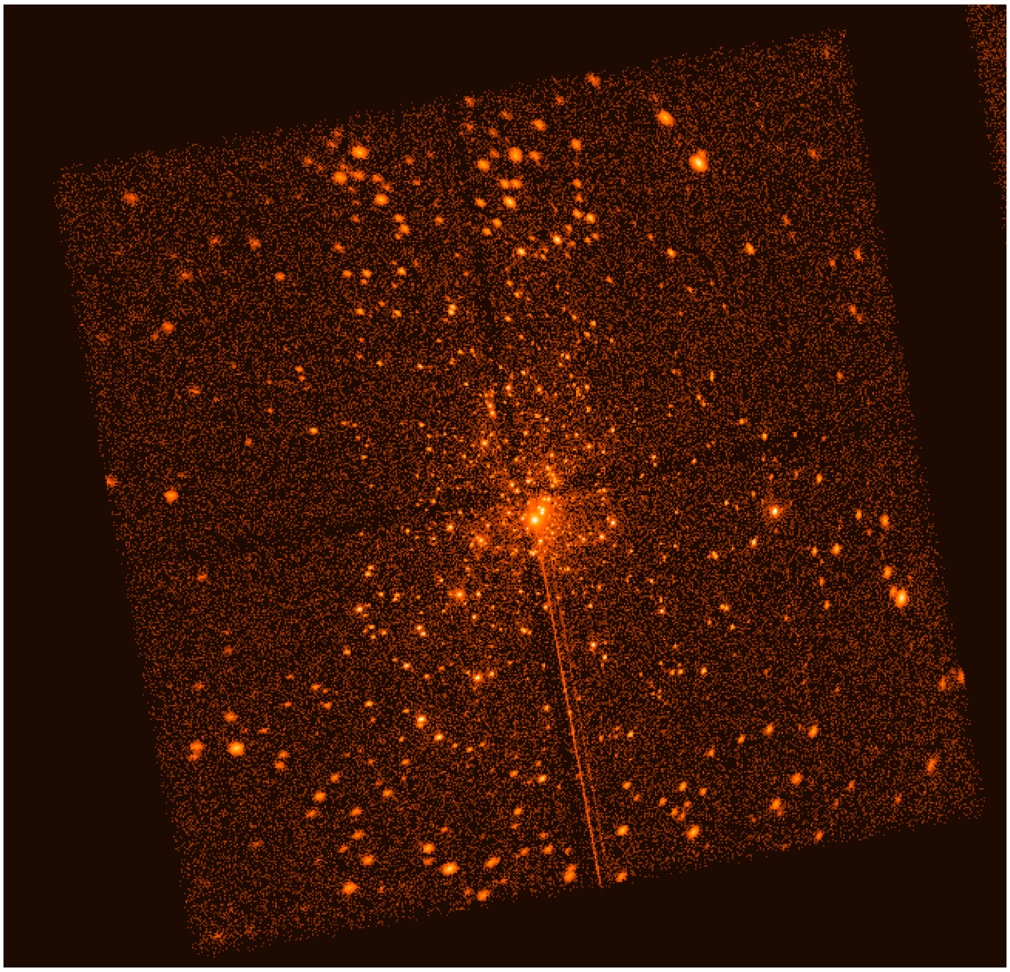

Figure 6. ACIS-I image of the Orion Nebula Cluster in the 0.2−8 keV band showing $\simeq$ 1000 X-ray sources. The $17' \times 17'$ array is shown here at a reduced resolution of $2'' \times 2''$ pixels. Intensity scaling is logarithmic according to the number of events. North is up and East is to left.

al., 1987) or so-called ProPlyDs (e.g. O'Dell & Wong, 1996) without stellar point sources. Objects of all masses ranging from the 50 $M_\odot$ star θ^1C Ori to those at or just below the 0.08 $M_\odot$ hydrogen burning limit are detected. As a reminder, the stars in this region are <1-3 Myr of age.

Comparison with an HR diagram complete in mass down to $\sim$0.1 $M_\odot$ for extinction $A_V < 2$ mag shows that Chandra/ACIS detected 91% of stars with $M/M_\odot > 0.3$ and 75% of those with $0.1 < M/M_\odot < 0.3$. Considering the deep near-infrared survey discussed above which is complete to $M/M_\odot > 0.02$ for $A_V < 10$ mag, most of the *stars* are detected although those with higher extinction generally are not detected and neither are substellar mass objects at any extinction. It is not known at present whether the lack of detection of candidate brown dwarf objects reflects a true astrophysical phenomenon or an L_X vs L_{bol} or L_X vs M relationship combined with the Chandra/ACIS limits.

Because Orion is a well-studied region, estimates for physical variables such as stellar masses, ages, radii, and rotational velocities exist for many hundreds of

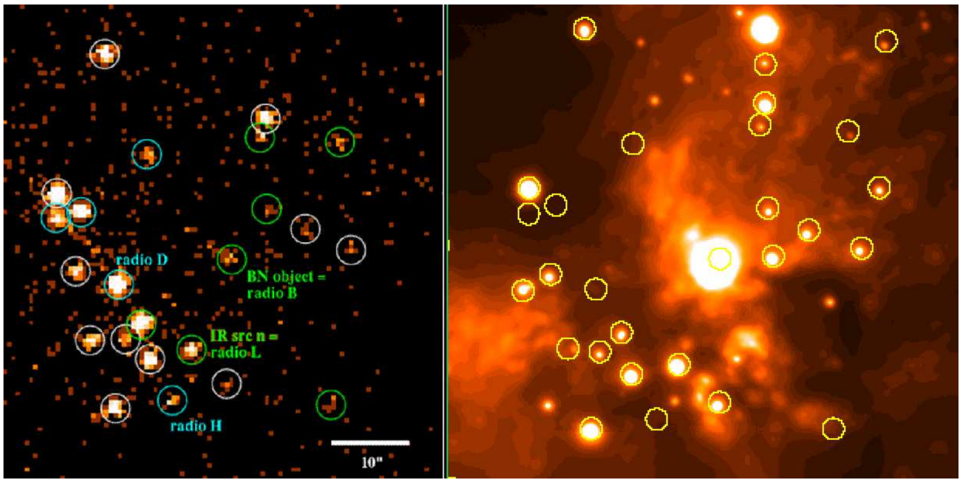

Figure 7. Comparison of x-ray and near-infrared images of the BN/KL region. The ACIS image is from 2-8 keV while the NIRC image is at 2μm. Circles in the left panel indicate hard x-ray sources while circles in the right panel indicate either hard or soft x-ray sources. Images are $\sim$1 x 1 arcmin^2 in size and centered on the BN object.

stars. Combination of these stellar parameters (and perhaps even circumstellar parameters such as disk accretion rates) with the Chandra x-ray data should enable sorting between various possibilities for the currently confounding genesis of x-ray activity in pre-main sequence stars. Thusfar our analysis has suggested a relatively constant level of L_X at early stages followed by development at older ages (corresponding to lower luminosities as the stars contract) of a large dispersion in x-ray activity for stars of the same mass and age.

Chandra/ACIS also gives us a clearer and deeper view into the BN/KL region which is embedded in molecular gas just behind the ONC, a site where massive star formation is currently taking place. In Fig. 7 we show a close-up of Fig. 6 comparing the ACIS-detected x-ray sources with the Keck/NIRC near-infrared sources. While the majority of x-ray sources over the full field of view of ACIS do have optical/infrared counterparts, the situation is slightly different in the BN/KL region. Source n is detected with ACIS, but the identification of the BN object with its closest X-ray neighbor ($\sim$ 0.3", i.e., 3σ separation) is unclear at the moment. The X-ray source may rather be associated with the BN extended circumstellar environment. IrC2, the third powerful embedded massive prototellar object in the region, is not detected. Several hard x-ray sources in the left panel do not have infrared counterparts in the right panel; most of these have been detected in the radio. For contrast, there are also a number of sources which are bright at K-band but which lack x-ray counterparts.

5. Concluding Remarks

Despite more than six decades of study of the Orion Nebula Cluster, we continue to learn new things about it with every improvement in technology. In some sense the Orion star-forming region is a prototype: it is the nearest Giant Molecular Cloud and the nearest region of recent massive star formation. As such, it is considered an important laboratory for testing our understanding of star formation processes in the Galaxy. Equally important, however, is discovering how typical Orion-like regions are in the Galaxy.

Acknowledgments. I would like to acknowledge my collaborators on these projects: Carpenter, Feigelson, Broos, Garmire, Pravdo, Townsley, and Tsuboi, without whom this presentation would not have been possible.

References

Baraffe, I., Chabrier, G., Allard, F., Hauschildt, P. H. 1998 AA 337, 403

Carpenter, J.M. 2001, AJ, in press.

Chini, R., Reipurth, B., Ward-Thompson, D., Bally, J., Nyman, L.-A., Sievers, A., & Billawala, Y. 1997, ApJ, 474, L135

Churchwell, E., Felli, M., Wood, D.O.S., & Massi, M. 1987, ApJ 321, 516

D'Antona F. and Mazzitelli, I. 1997, in Cool Stars in Clusters and Associations, eds. G. Micela and R. Pallavicini, Mem. S. A. It., 68, 807

D'Antona F. and Mazzitelli, I. 1998, private communication

Feigelson, E.D. & Montmerle, T. 1999, ARAA 37, 363

Feigelson, E.D. et al., 2000, in preparation

Felli, M., Churchwell, E., Wilson, T., & Taylor, G.B. 1993, AAS 98, 137

Garmire, G., Feigelson, E.D., Broos, P., Hillenbrand, L.A., Pravdo, S.H., Townsley, L., & Tsuboi, Y. 2000, AJ, 120, 1426

Goldsmith, P. F., Bergin, E. A., & Lis, D. C. 1997, ApJ, 493, 615

Hillenbrand, L.A., 1997, AJ, 113, 1733

Hillenbrand, L.A. & Carpenter, J.M. 2000, ApJ 540, 236

Hillenbrand, L.A. & Hartmann, L.W. 1998 ApJ 492, 540

Hillenbrand, L.A., Strom, S.E., Calvet, N., Merrill, K.M., Gatley, I., Makidon, R.M., Meyer, M.R., & Skrutskie, M.F. 1998 AJ, 116, 1816

Johnstone, D., & Bally, J. 1999, ApJ 510, L49

Lada, E.A., DePoy, D.L., Evans, N.J., & Gatley, I. 1991, ApJ, 371, 171

Lucas & Roche, 2000, MNRAS, submitted

Luhman, K.L., Rieke, G.H., Young, E.T., Cotera, A.S., Chen, H., Rieke, M.J., Schneider, G., & Thompson, R.I. 2000, ApJ, 540, 1016

McCaughrean, M.J., Burkert, A., & O'Dell, C.R. 2001, "The Orion Complex, Revisted"

Menten, K. et al., private communication

O'Dell, C.R. & Wong, S.K. 1996, AJ 111, 846

Palla, F. & Stahler, S.W. 1999, ApJ 525, 772,

Prosser, C.F., Stauffer, J.R., Hartmann, L.W., Soderblom, D.R., Jones, B.F., Werner, M.W., & McCaughrean, M.J. 1994 ApJ 421, 517

Simon, M., Close, L.M.& Beck, T.L. 1999, AJ 117, 1375

Strom, K.M., Strom, S.E., & Merrill, K.M. 1993 ApJ 412, 233

Siess, L., Dufour, E., & Forestini, M. 2000, AA 358, 593